The activation and transformations of acenaphthylene by osmium carbonyl cluster complexes

Richard D. Adams *, Burjor Captain, Jack L. Smith, Jr.

Department of Chemistry and Biochemistry, University of South Carolina, 631 Sumter Street GRSC 109, Columbia, SC 29208, USA

Abstract

The reaction of $Os_3(CO)_{10}(NCMe)_2$ (1) with an excess of acenaphthylene at room temperature provided the complex $Os_3(CO)_{10}(\mu-H)(\mu-\eta^2-C_{12}H_7)$ (2). Compound 2 contains a $\sigma-\pi$ coordinated acenaphthyl ligand bridging an edge of the cluster. Compound 2 was converted to the complex $Os_3(CO)_9(\mu-H)_2(\mu_3-\eta^2-C_{12}H_6)$ (3) when heated to reflux in a cyclohexane solution. Compound 3 contains a triply bridging acenaphthyne ligand. Compound 3 reacts with acenaphthylene again at 160 °C to yield four new cluster complexes: $Os_4(CO)_{12}(\mu_4-\eta^2:\eta^2-C_{12}H_6)$ (4); $Os_2(CO)_6(\mu-\eta^4-C_{24}H_{12})$ (5); $Os_3(CO)_9(\mu-H)(\mu_3-\eta^4-C_{24}H_{13})$ (6); and $Os_2(CO)_5(\mu-\eta^4-C_{24}H_{12})(\eta^2-C_{12}H_8)$ (7). All compounds were characterized crystallographically. Compound 4 is a butterfly cluster of four osmium atoms bridged by a single acenaphthyne ligand. Compounds 5 and 7 are dinuclear osmium clusters containing metallacycles formed by the coupling of two equivalents of acenaphthyne. Compound 6 is a triosmium cluster formed by the coupling of an acenaphthyne ligand to an acenapthyl group that is coordinated to the cluster through a combination of σ and π-bonding.
© 2003 Elsevier B.V. All rights reserved.

Keywords: Acenaphthylene; Acenapthyne; Osmium; C–C Coupling

1. Introduction

It well known that arene molecules can act as ligands in organometallic compounds [1–3]. These ligands typically coordinate through an η^6-bonding mode to one metal atom or through $\mu_3-\eta^2:\eta^2:\eta^2$ bridging coordination to a triangular group of three metal atoms [4]. Aryne ligands, such as benzyne containing an internal triple bond, are highly unstable, but can be isolated when they are coordinated to one or more transition metal atoms [5,6]. These ligands can be formed by cleavage of hydrogen atoms or substituents from substituted phenyl rings [7–15]. Arynes stabilized by osmium cluster compounds include $Os_3(CO)_9(\mu_3-\eta^2-C_6H_4)$ [8], $Os_4(CO)_{12}(\mu_4-\eta^2:\eta^2-C_6H_4-C_6H_5)$, and $Os_2(CO)_6(\mu-\eta^4-C_{12}H_{10})$ [9], (see Fig. 1). C–H activation by osmium cluster complexes on compounds containing unsaturated 5-membered rings can lead to triply brid-

ging cyclopentyne and related ligands: $Os_3(CO)_9(\mu-H)_2(\mu_3-\eta^2-C_7H_8)$ [16]; $Os_4(CO)_9(\mu-H)(\eta^5-C_9H_7)(\mu_3-\eta^2-C_9H_6)$ [17]; $Os_3(CO)_9(\mu-H)(\mu_3-\eta^2-C_4H_2NCH_3)$ [18]; and $Os_3(CO)_9(\mu-H)_2(\mu_3-\eta^2-C_6SH_4)$ [19].

Metal clusters are also known to facilitate the dimerization and trimerization of alkynes [20]. The osmium–acetylene complex $Os_3(CO)_9(\mu-H)_2(PhC_2Ph)$ reacts with PhC_2Ph to give the compound $Os_3(CO)_9(C_4Ph_4)$ which contains a metallacyclopentadiene ring. Further reaction with an additional equivalent of PhC_2Ph introduces another μ_3-alkyne and eventually leads to hexaphenylbenzene by additional coupling. The reactions of acenaphthylene with $Fe_3(CO)_{12}$ and $Ru_3(CO)_{12}$ yield the complexes, $Fe_2(CO)_5(\mu-\eta^8-C_{12}H_8)$ [21] and $Ru_3(CO)_7(\mu-\eta^{10}-C_{12}H_8)$ [22], respectively, both of which contain π-coordinated acenaphthylene ligands.

Herein, we show that $Os_3(CO)_{10}(NCMe)_2$ reacts with acenaphthylene preferentially by activation of the two CH bonds on the five membered ring in a series of two steps that leads to the complexes $Os_3(CO)_{10}(\mu-H)(\mu-\eta^2-C_{12}H_7)$ (2) and $Os_3(CO)_9(\mu_3-\eta^2-C_{12}H_6)(\mu-H)_2$ (3). The

* Corresponding author. Tel.: +1-803-7777187; fax: +1-803-7776781.
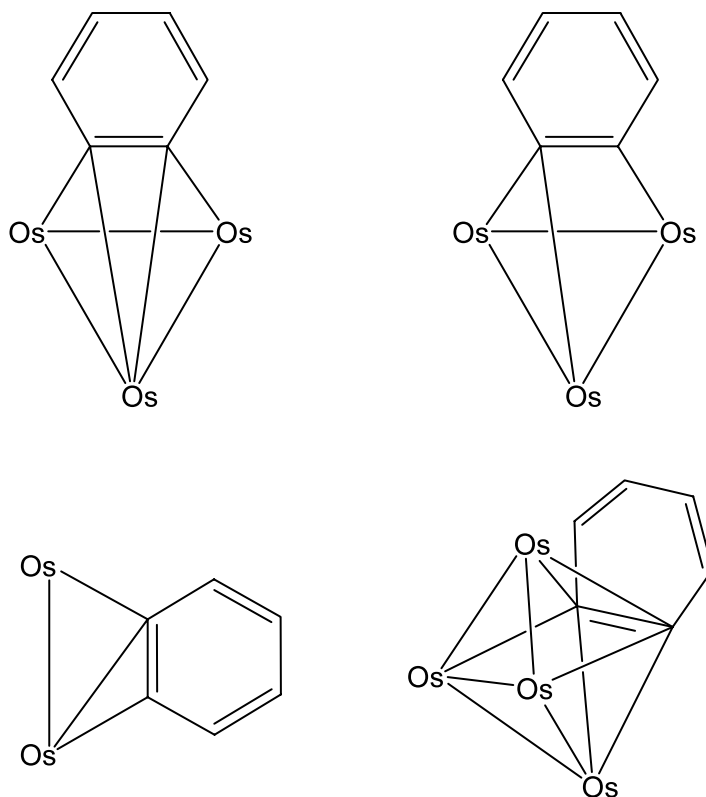*E-mail address:* adams@mail.chem.sc.edu (R.D. Adams).

Fig. 1. Bonding modes of benzyne to two, three, and four osmium atoms.

latter contains a triply bridging acenaphthyne ligand. Compound **3** reacts further with acenaphthylene by CH activation and C–C bond formation to yield products containing coupled acenaphthylene groupings that bridge the metal atoms. These processes could represent some of the first steps in the coupling of polycyclic aromatic compounds to produce, bucky bowls, C_{60}, and/or carbon nanotubes [23]. Precursors to these compounds such as decacyclene ($C_{36}H_{18}$) are the result of the aggregation of smaller arenes. Decacyclene can be produced by the reaction of acenaphthylene with elemental sulfur at 300 °C [24] or via the trimerization of acenaphthenequinone by a zero-valent titanium catalyst [25].

2. Experimental

2.1. General data

All reactions were performed under a nitrogen atmosphere. Reagent grade solvents were dried by the standard procedures and were freshly distilled prior to use. Infrared spectra were recorded on an Avatar 360 FTIR spectrophotometer. ^{1}H-NMR spectra were recorded on a Varian Inova 300 spectrometer operating at 300.08 MHz. Elemental analyses were performed by Desert Analytics (Tucson, AZ). Mass spectra were recorded on a VG70SQ mass spectrometer. Acenaphthylene (75%) was purchased from Aldrich Chemical Company and used without further purification. $Os_3(CO)_{10}(NCMe)_2$ (**1**) was prepared according to published procedures [26]. Product separations were performed by TLC in air on Analtech 0.25, 0.5, and 1.0 mm silica gel 60 Å F254 glass plates.

2.1.1. Synthesis of $Os_3(CO)_{10}(\mu\text{-}H)(\mu-\eta^2\text{-}C_{12}H_7)$ (2)

Compound **1** (15.0 mg, 0.016 mmol) was added to a solution of acenaphthylene (16.5 mg, 0.081 mmol) in 15 ml CH_2Cl_2. The color of the reaction mixture immediately changed from yellow to orange. The mixture was stirred at room temperature (r.t.) for 5 min. The solvent was removed in vacuo and the product was isolated by TLC by using pure hexane to give 11.2 mg of orange $Os_3(CO)_{10}(\mu\text{-}H)(\mu-\eta^2\text{-}C_{12}H_7)$ (**2**) in 69% yield. Spectral data for **2**: IR ν_{CO} (cm^{-1} in hexane): 2099 (m), 2071 (w), 2053 (s), 2023 (s), 2010 (s), 2003 (s), 1983 (m), 1974 (m), 1950 (w). ^{1}H-NMR (CDCl$_3$): $\delta = 7.4$–8.1 (m, 7H), -15.65 (s, 1H, hydride). Anal. Calc. C, 26.34; H, 0.81. Found: C, 26.60; H, 0.92%.

2.1.2. Synthesis of $Os_3(CO)_9(\mu\text{-}H)_2(\mu_3-\eta^2\text{-}C_{12}H_6)$ (3)

Compound **1** (26.9 mg, 0.029 mmol) was added to a refluxing solution of acenaphthylene (29.3 mg, 0.144 mmol) in 15 ml cyclohexene. The color of the reaction mixture immediately changed from yellow to orange,

then to dark brown and finally back to yellow. After 2 h the reaction mixture was cooled. The solvent was removed in vacuo, and the product isolated by TLC by using pure hexane to give 19.0 mg of yellow $Os_3(CO)_9(\mu\text{-H})_2(\mu_3\text{-}\eta^2\text{-}C_{12}H_6)$ (3) in 67% yield. Spectral data for 3: IR ν_{CO} (cm^{-1} in hexane): 2108 (m), 2081 (vs), 2058 (vs), 2035 (s), 2023 (m), 2011 (s), 2002 (m), 1986 (m). ^{1}H-NMR (CDCl$_3$, ppm at -80 °C): $\delta = 7.80$ (d, 2H), 7.62 (d, 2H), 7.54 (t, 2H), -17.08 (s, 1H), -21.05 (s, 1H). Anal. Calc. C, 25.87; H, 0.83. Found: C, 26.15; H, 0.83%.

2.1.3. Conversion of 2 to 3

Twenty milligrams, 0.020 mmol of 2 was dissolved in 15 ml cyclohexane and heated to reflux. After 2 h the reaction mixture was cooled, the solvent removed in vacuo, and the product isolated by TLC by using pure hexane to give 15.4 mg of 3 in 79% yield.

2.1.4. Reaction of 3 with acenaphthylene

37.7 mg, 0.038 mmol of 3 and 78.5 mg, 0.387 mmol of acenaphthylene were dissolved in 20 ml octane and placed in a stainless steel *Parr* pressure reactor. The reactor was sealed and placed in an oil bath maintained at 160 °C for 8 h. After cooling the solvent was removed in vacuo, and the products were isolated by TLC by using a 3:1 mixture of hexane–CH$_2$Cl$_2$ to yield in order of elution 5.5 mg of orange $Os_4(CO)_{12}(\mu_4\text{-}\eta^2:\eta^2\text{-}C_{12}H_6)$ (4), 11% yield; 4.3 mg of yellow $Os_2(CO)_6(\mu\text{-}\eta^4\text{-}C_{24}H_{12})$ (5), 13% yield; 1.8 mg of yellow-orange $Os_3(CO)_9(\mu\text{-H})(\mu_3\text{-}\eta^4\text{-}C_{24}H_{13})$ (6), 4% yield; and 1.1 mg of yellow $Os_2(CO)_5(\mu\text{-}\eta^4\text{-}C_{24}H_{12})(\eta^2\text{-}C_{12}H_8)$ (7), 3% yield. Spectral data for 4: IR ν_{CO} (cm^{-1} in hexane): 2098 (w), 2073 (vs), 2048 (s), 2040 (s), 2014 (m), 2004 (m), 1976 (w). Compound 4: ^{1}H-NMR (CDCl$_3$): $\delta = 7.61$ (d, 2H), 7.41–7.50 (m, 4H). Anal. Calc. C, 23.11; H, 0.49. Found: C, 24.38; H, 0.57%. MS (DEP) m/z $1248-n(28)$, $n = 0$–12 (M$^+$ $-n$(CO)). Spectral data for 5: IR ν_{CO} (cm^{-1} in hexane): 2078 (m), 2051 (vs), 2012 (m), 2004 (m), 1976 (m). Compound 5: ^{1}H-NMR (CDCl$_3$): $\delta = 8.54$ (d, 4H), 8.15 (d, 4H), 7.94 (t, 4H, Ph); MS (DEP) m/z $850-n(28)$, $n = 0$–6 (M$^+$ $-n$(CO)), 340 (Os(C$_{12}$H$_6$)$^+$). Spectral data for 6: IR ν_{CO} (cm^{-1} in hexane): 2089 (s), 2062 (vs), 2041 (vs), 2034 (m), 2017 (m), 2013 (w), 1994 (w), 1987 (w). Compound 6: ^{1}H-NMR (CDCl$_3$): $\delta = 7.5$–7.9 (m, 12H), 4.19 (d, 1H, $^3J_{H-H} = 1.5$ Hz), -18.09 (d, 1H, hydride, $^3J_{H-H} = 1.5$ Hz). MS (DEP) m/z $1126-n(28)$, $n = 0$–9 (M$^+$ $-n$(CO)). Spectral data for 7: IR ν_{CO} (cm^{-1} in hexane): 2062 (vs), 2027 (m), 1993 (s), 1976 (m), 1971 (w). ^{1}H-NMR (CDCl$_3$): $\delta = 7.5$–8.5 (m, 14H).

2.1.5. Conversion of 6 to 5

Two milligrams, 0.0018 mmol of 6 was dissolved in 5 ml octane and placed in a stainless steel *Parr* pressure reactor. The reactor was sealed and placed in an oil bath maintained at 160 °C for 5 h. After cooling the solvent was removed in vacuo and the product was isolated by TLC by using a 3:1 mixture of hexane–CH$_2$Cl$_2$ to yield 0.6 mg of 5 in 40% yield.

2.1.6. Crystallographic analyses

Orange crystals of 2, red crystals of 4, and yellow crystals of 5, 6, and 7 suitable for diffraction analysis were grown by slow evaporation of solvent from a hexane–methylene chloride solvent mixture at 5 °C. Yellow crystals of 3 were grown by slow evaporation of cyclohexane at 25 °C. Each crystal was glued onto the end of a thin glass fiber. X-ray intensity data were measured using a Bruker SMART APEX CCD-based diffractometer using Mo–K$_\alpha$ radiation ($\lambda = 0.71073$ Å). The raw data frames were integrated with the SAINT+ program using a narrow-frame integration algorithm [27]. Corrections for the Lorentz and polarization effects were also applied by using the program SAINT. An empirical absorption correction based on the multiple measurement of equivalent reflections was applied by using the program SADABS. All structures were solved by a combination of direct methods and difference Fourier syntheses, and refined by full-matrix least squares on F^2, by using the SHELXTL software package [28]. Crystal data, data collection parameters, and results of the analyses for compounds 2, 3, and 4 are given in Table 1. Data for compounds 5, 6, and 7 are given in Table 2. All non-hydrogen atoms were refined with anisotropic displacement parameters. Hydrogen atoms were placed in geometrically idealized positions and included as standard riding atoms.

Compound 2 crystallized in the monoclinic crystal system. The space group $P2_1/n$ was identified uniquely on the basis of the systematic absences in the intensity data. The hydride ligand was located and refined with an isotropic displacement parameter.

Compound 3 crystallized in the monoclinic crystal system. The systematic absences in the data were consistent with the space groups $C2/c$ or Cc. Cc was selected. There are two independent formula equivalents of the complex in the asymmetric unit. Atom C(81) was refined with an isotropic displacement parameter because it gave a negative thermal parameter when refined anisotropically.

Compounds 4 and 5 crystallized in the monoclinic crystal system. The space group $P2_1/n$ was identified uniquely on the basis of the systematic absences in the intensity data.

Compound 6 crystallized in the triclinic crystal system. The space group $P\bar{1}$ was assumed and confirmed by the successful solution and refinement of the structure. The hydride ligand was located and refined with an isotropic displacement parameter.

Compound 7 crystallized in the orthorhombic crystal system. The space group *Pbca* was established on the

Table 1
Crystallographic data for compounds **2**, **3**, and **4**

	2	**3**	**4**
Empirical formula	$C_{22}H_8O_{10}Os_3$	$C_{42}H_{12}O_{18}Os_6$	$C_{24}H_6O_{12}Os_4$
Formula weight	1002.88	1945.72	1247.09
Temperature (K)	296	296	296
Crystal system	Monoclinic	Monoclinic	Monoclinic
Space group	$P2_1/n$	Cc	$P2_1/n$
Lattice parameters			
a (Å)	8.6536(3)	7.7099(4)	8.9814(4)
b (Å)	24.9550(10)	16.2851(9)	17.6417(7)
c (Å)	10.5601(4)	36.159(2)	16.3928(7)
α (°)	90	90	90
β (°)	92.9680(10)	92.9930(10)	92.4190(10)
γ (°)	90	90	90
V (Å^3)	2277.40(15)	4533.8(4)	2595.08(19)
Z-value	4	4	4
ρ_{calc} (g cm^{-3})	2.925	2.851	3.192
μ (Mo–K$_\alpha$) (mm^{-1})	16.753	16.822	19.586
$2\theta_{max}$ (°)	56.60	53.16	56.18
Observations	4831	8108	5485
Parameters	344	590	361
Maximum shift in cycle	0.001	0.002	0.001
Max/min	1.000/0.524	1.000/0.675	1.000/0.312
Residuals [a]: R_1; wR_2 ($I > 2\sigma(I)$)	0.0229; 0.0487	0.0467; 0.1127	0.0371; 0.0956
Absorption correction	SADABS	SADABS	SADABS
Goodness-of-fit on F^2	1.019	1.18	1.02
Largest peak in final difference map (e Å^{-3})	0.873	2.042	4.248

[a] $R = \Sigma_{hkl}(||F_{obs}| - |F_{calc}||)/\Sigma_{hkl}|F_{obs}|$; $R_w = [\Sigma_{hkl} w(|F_{obs}| - |F_{calc}|)^2/\Sigma_{hkl} wF_{obs}^2]^{1/2}$; $w = 1/\sigma^2(F_{obs})$; GOF $= [\Sigma_{hkl} w(|F_{obs}| - |F_{calc}|)^2/(n_{data} - n_{vari})]^{1/2}$.

Table 2
Crystallographic data for compounds **5**, **6**, and **7**

	5	**6**	**7**
Empirical formula	$C_{30}H_{12}O_6Os_2$	$C_{33}H_{14}O_9Os_3$	$C_{41}H_{20}O_5Os_2 \cdot CH_2Cl_2$
Formula weight	848.80	1125.04	1057.90
Temperature (K)	296	296	296
Crystal system	Monoclinic	Triclinic	Orthorhombic
Space group	$P2_1/n$	$P\bar{1}$	$Pbca$
Lattice parameters			
a (Å)	8.6687(4)	7.6235(3)	14.1787(10)
b (Å)	19.6308(9)	12.1658(6)	21.1084(14)
c (Å)	14.5350(7)	16.7664(9)	22.7258(15)
α (°)	90	96.0690(10)	90
β (°)	101.1900(10)	102.9670(10)	90
γ (°)	90	103.2750 (10)	90
V (Å^3)	2426.4(2)	1454.46(12)	6801.7(8)
Z-value	4	2	8
ρ_{calc} (g cm^{-3})	2.323	2.569	2.066
μ (Mo–K$_\alpha$) (mm^{-1})	10.509	13.129	7.67
$2\theta_{max}$ (°)	56.56	56.60	50.06
Observations	4652	5917	4606
Parameters	343	410	460
Maximum shift in cycle	0.002	0.002	0.001
Max/min	1.0/0.719	1.0/0.623	1.0/0.777
Residuals [a]: R_1; wR_2 ($I > 2\sigma(I)$)	0.0347; 0.0688	0.0386; 0.0862	0.0489; 0.0893
Absorption correction	SADABS	SADABS	SADABS
Goodness-of-fit on F^2	0.982	1.104	1.113
Largest peak in final difference map (e Å^{-3})	2.102	1.751	1.636

[a] $R = \Sigma_{hkl}(||F_{obs}| - |F_{calc}||)/\Sigma_{hkl}|F_{obs}|$; $R_w = [\Sigma_{hkl} w(|F_{obs}| - |F_{calc}|)^2/\Sigma_{hkl} wF_{obs}^2]^{1/2}$; $w = 1/\sigma^2(F_{obs})$; GOF $= [\Sigma_{hkl} w(|F_{obs}| - |F_{calc}|)^2/(n_{data} - n_{vari})]^{1/2}$.

basis of the systematic absences observed during the collection of the intensity data. One molecule of CH_2Cl_2 from the crystallization solvent cocrystallized with the complex. The CH_2Cl_2 molecule was located and refined with anisotropic displacement parameters.

3. Results and discussion

The reaction of $Os_3(CO)_{10}(NCMe)_2$ (**1**) with an excess of acenaphthylene at room temperature provided the complex $Os_3(CO)_{10}(\mu\text{-H})(\mu\text{-}\eta^2\text{-}C_{12}H_7)$ (**2**) in 69% yield. When heated to reflux in cyclohexane for 2 h, compound **2** was converted to the new compound $Os_3(CO)_9(\mu\text{-H})_2(\mu_3\text{-}\eta^2\text{-}C_{12}H_6)$ (**3**) in 79% yield. Compound **3** can also be obtained in one step in 67% yield by the reaction of **1** with an excess of acenaphthylene in refluxing cyclohexane for 2 h. Compounds **2** and **3** were both characterized by IR, NMR, elemental, and single crystal X-ray diffraction analyses. An ORTEP diagram of the molecular structure of **2** is shown in Fig. 2. Selected bonds distances and angles for compound **2** are given in Table 3. Compound **2** contains an acenaphthyl ligand coordinated to the Os(1)–Os(2) edge of the cluster through the well-known σ–π coordination mode [20]. The Os(1)–Os(2) bond is also bridged by a hydride ligand, $\delta = -15.65$ ppm in the ¹H-NMR spectrum. The Os(1)–Os(2) bond is slightly shorter than the other two metal–metal bonds (Os(1)–Os(2) = 2.8349(2), Os(1)–Os(3) = 2.8799(3), Os(2)–Os(3) = 2.8768(2) Å), due to the presence of the bridging ligand. Compound **2** is formed by the activation of one of the C–H bonds of the five membered ring of acenaphthylene by the triangular osmium metal cluster. The two NCMe ligands were displaced from **1**, but there was no loss of CO and the reaction is complete within 5 min.
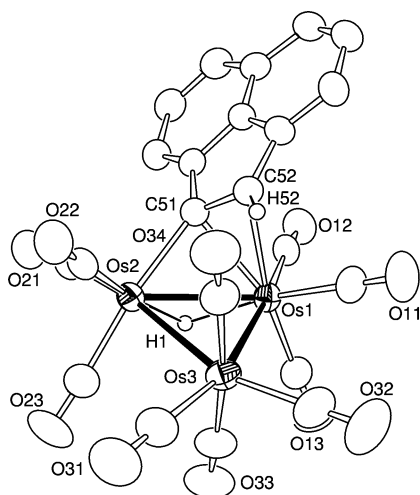
Table 3
Selected intramolecular distances and angles for compounds **2** and **3** [a]

Compound **2**		Compound **3**	
Bond distances (Å)			
Os(1)–Os(2)	2.8349(2)	Os(1)–C(51)	2.285(18)
Os(1)–Os(3)	2.8768(2)	Os(1)–C(52)	2.289(15)
Os(2)–Os(3)	2.8799(3)	Os(1)–Os(3)	2.7645(10)
Os(1)–C(51)	2.319(4)	Os(1)–Os(2)	2.8667(10)
Os(1)–C(52)	2.507(4)	Os(2)–C(51)	2.11(2)
Os(2)–C(51)	2.140(4)	Os(2)–Os(3)	3.0781(10)
Os(1)–H(1)	1.87(4)	Os(3)–C(52)	2.076(17)
Os(2)–H(1)	1.75(4)	C(51)–C(52)	1.44(3)
C(51)–C(52)	1.391(6)	C–O (av)	1.15(1)
C–O (av)	1.13(1)		
Bond angles (°)			
C(51)–Os(1)–Os(2)	47.79(10)	C(51)–Os(1)–Os(3)	73.1(6)
C(52)–Os(1)–Os(2)	73.49(10)	C(52)–Os(1)–Os(3)	47.4(4)
C(51)–Os(1)–Os(3)	90.43(10)	C(51)–Os(1)–Os(2)	46.7(5)
C(52)–Os(1)–Os(3)	87.79(10)	C(52)–Os(1)–Os(2)	67.2(4)
Os(2)–Os(1)–Os(3)	60.552(6)	Os(3)–Os(1)–Os(2)	66.24(3)
Os(2)–Os(1)–H(1)	36.8(14)	C(51)–Os(2)–Os(1)	52.0(5)
Os(3)–Os(1)–H(1)	80.0(13)	C(51)–Os(2)–Os(3)	68.6(7)
C(51)–Os(2)–Os(1)	53.37(11)	Os(1)–Os(2)–Os(3)	55.29(2)
C(51)–Os(2)–Os(3)	94.09(11)	C(52)–Os(3)–Os(1)	54.2(4)
Os(1)–Os(2)–Os(3)	60.443(6)	C(52)–Os(3)–Os(2)	64.9(5)
Os(1)–Os(2)–H(1)	39.9(15)	Os(1)–Os(3)–Os(2)	58.47(2)
Os(3)–Os(2)–H(1)	81.8(14)	Os–C–O (av)	176(1)
Os(1)–Os(3)–Os(2)	59.004(6)		
Os–C–O (av)	176(1)		

[a] Estimated S.D.s in the least significant figure are given in parenthesis.

An ORTEP diagram of the molecular structure of **3** is shown in Fig. 3. Selected bonds distances and angles for **3** are given in Table 3. This compound contains a triply bridging acenaphthyne ligand which has adopted the usual di σ+π coordination mode [4,20]. There are two bridging hydride ligands. They were not located directly, but are believed to bridge the two long Os(1)–Os(2) and Os(2)–Os(3) metal–metal bonds: 2.8667(10), 3.0781(10) Å bonds. At room temperature, there is only a single

Fig. 2. An ORTEP diagram of the molecular structure of $Os_3(CO)_{10}(\mu\text{-}H)(\mu\text{-}\eta^2\text{-}C_{12}H_7)$ (**2**) showing 40% thermal ellipsoid probability.
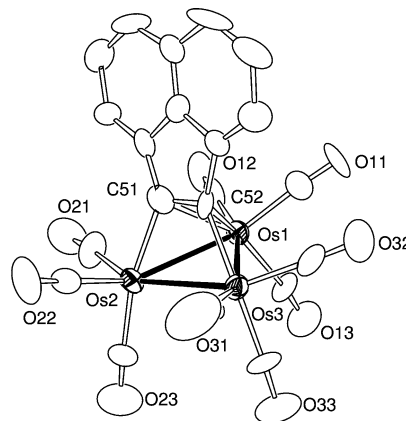

Fig. 3. An ORTEP diagram of the molecular structure of $Os_3(CO)_9(\mu\text{-}H)_2(\mu_3\text{-}\eta^2\text{-}C_{12}H_6)$ (**3**) showing 40% thermal ellipsoid probability. The hydride ligands were not located and are not shown.

broad resonance at -19.0 ppm for the hydride ligands in the ^{1}H-NMR spectrum. This is due to a dynamical exchange process that averages the ligands between the two sites. This was confirmed by low temperature ^{1}H-NMR measurements. At $-80\,^\circ$C the two separate hydride resonances were observed at $\delta = -17.08$ and -21.05 ppm. Both resonances broadened, reversibly, and coalesced at $-5\,^\circ$C when the temperature was raised. From the coalescence temperature we have calculated the free energy of activation for the exchange process, $\Delta G^{\ddagger}_{268} = 11.2$ kcal mol^{-1}. These properties are similar to that of the known osmium–benzyne complex Os$_3$(CO)$_9$(μ-H)$_2$(C$_6$H$_4$) [8]. Compound **3** is formed from **2** by the loss of one CO ligand and the cleavage of the alkenyl C–H bond, and thus requires a higher temperature (80 $^\circ$C) and longer reaction time (2 h) (see Scheme 1).

Compound **3** reacts with an additional quantity of acenaphthylene at 160 $^\circ$C over a period of 8 h to give four products that have been identified as: Os$_4$(CO)$_{12}$($\mu_4-\eta^2$:η^2-C$_{12}$H$_6$) (**4**); Os$_2$(CO)$_6$($\mu-\eta^4$-C$_{24}$H$_{12}$) (**5**); Os$_3$(CO)$_9$(μ-H)($\mu_3-\eta^4$-C$_{24}$H$_{13}$) (**6**); and Os$_2$(CO)$_5$($\mu-\eta^4$-C$_{24}$H$_{12}$)(η^2-C$_{12}$H$_8$) (**7**) in 11, 13, 4, and 3% yields, respectively (see Fig. 4). All four products were characterized by IR, NMR, mass spectra, and single crystal X-ray diffraction analyses. An ORTEP diagram of **4** is shown in Fig. 5. Selected bonds distances and angles for compound **4** are shown in Table 4. Compound **4** contains a butterfly cluster of four osmium atoms bridged by an acenaphthyne ligand. As expected, the Os(2)–Os(3) bond (the 'hinge' of the butterfly) is slightly longer than the other metal–metal bonds (Os(2)–Os(3) = 2.9094(4), Os(1)–Os(2) = 2.7691(4),
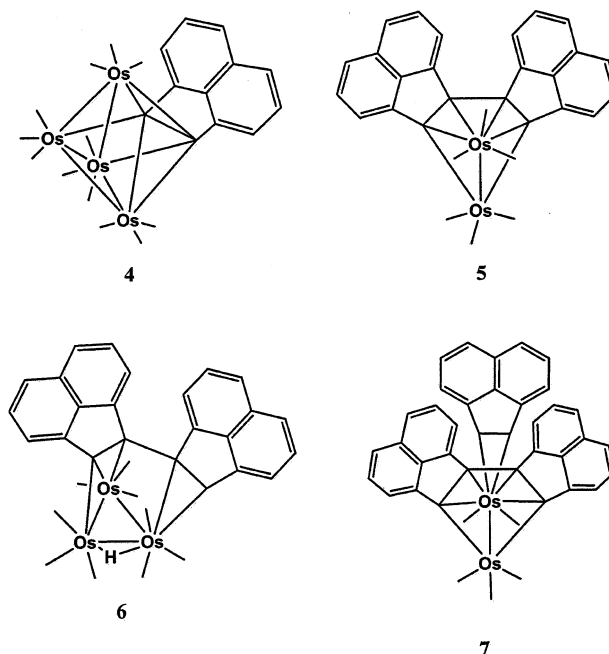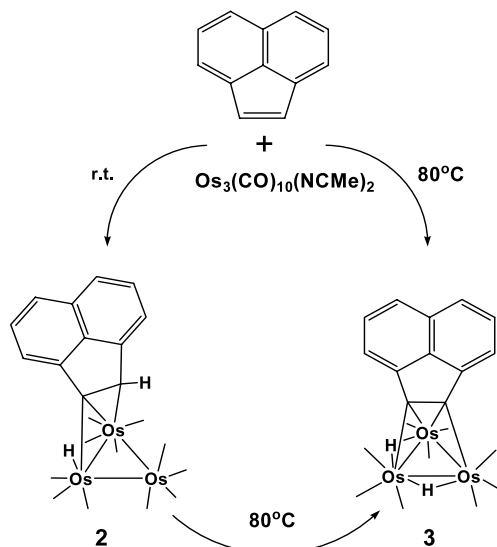

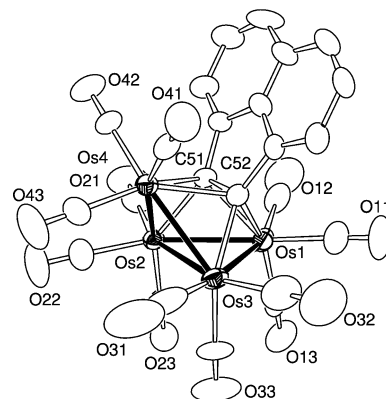Fig. 4. Products formed from the reaction of **3** with acenaphthylene at 160 $^\circ$C.

Fig. 5. An ORTEP diagram of the molecular structure of Os$_4$(CO)$_{12}$($\mu_4-\eta^2$:η^2-C$_{12}$H$_6$) (**4**) showing 40% thermal ellipsoid probability.

Os(1)–Os(3) = 2.7729(4), Os(2)–Os(4) = 2.7495(4), Os(3)–Os(4) = 2.7645(4) Å. The C–C distance of the formal C–C triple bond C(51)–C(52) is also very long 1.501(9) Å, as expected because of its coordination to four metal atoms.

An ORTEP diagram of **6** is shown in Fig. 6. Selected bonds distances and angles for compound **6** are shown in Table 4. Compound **6** contains two acenaphthyl groups that have been coupled by formation of a C–C

Scheme 1.

Table 4
Selected intramolecular distances and angles for compounds 4 and 6 [a]

Compound 4		Compound 6	
Bond distances (Å)			
Os(1)–C(51)	2.242(7)	Os(1)–Os(2)	2.7632(4)
Os(1)–C(52)	2.261(7)	Os(1)–Os(3)	2.9016(4)
Os(1)–Os(2)	2.7691(4)	Os(2)–Os(3)	2.9818(5)
Os(1)–Os(3)	2.7729(4)	Os(2)–H(1)	1.61(7)
Os(2)–C(51)	2.123(7)	Os(3)–H(1)	1.89(7)
Os(2)–Os(4)	2.7495(4)	Os(1)–C(51)	2.295(7)
Os(2)–Os(3)	2.9094(4)	Os(1)–C(52)	2.322(7)
Os(3)–C(52)	2.128(7)	Os(2)–C(51)	2.093(8)
Os(3)–Os(4)	2.7645(4)	Os(3)–C(54)	2.333(8)
Os(4)–C(51)	2.256(7)	Os(3)–C(53)	2.457(8)
Os(4)–C(52)	2.259(7)	C–O (av)	1.13(1)
C(51)–C(52)	1.501(9)		
C–O (av)	1.12(1)		
Bond angles (°)			
Os(1)–Os(2)–Os(3)	58.397(10)	Os(1)–Os(2)–Os(3)	60.531(11)
Os(1)–Os(3)–Os(2)	58.270(10)	Os(1)–Os(3)–Os(2)	56.005(10)
Os(2)–Os(1)–Os(3)	63.333(10)	Os(2)–Os(1)–Os(3)	63.465(11)
Os(2)–Os(4)–Os(3)	63.691(11)	Os(1)–Os(2)–H(1)	92(2)
Os(4)–Os(2)–Os(3)	58.404(10)	Os(3)–Os(2)–H(1)	34(2)
Os(4)–Os(2)–Os(1)	92.207(11)	Os(1)–Os(3)–H(1)	82(2)
Os(4)–Os(3)–Os(2)	57.905(10)	Os(2)–Os(3)–H(1)	29(2)
Os(4)–Os(3)–Os(1)	91.806(12)	C(51)–Os(1)–Os(2)	47.79(19)
C(51)–Os(1)–Os(2)	48.74(18)	C(51)–Os(2)–Os(3)	82.1(2)
C(51)–Os(4)–Os(3)	71.87(19)	C(52)–Os(1)–Os(2)	78.0(2)
C(52)–Os(1)–Os(2)	72.03(17)	C(53)–Os(3)–Os(1)	66.09(18)
C(52)–Os(1)–Os(3)	48.71(18)	C(53)–Os(3)–Os(2)	86.01(18)
C(52)–Os(4)–Os(3)	48.86(19)	C(54)–Os(3)–Os(1)	97.2(2)
Os–C–O (av)	178(1)	Os–C–O (av)	177(1)

[a] Estimated S.D.s in the least significant figure are given in parentheses.

Fig. 6. An ORTEP diagram of the molecular structure of $Os_3(CO)_9(\mu-H)(\mu_3-\eta^4-C_{24}H_{13})$ (6) showing 40% thermal ellipsoid probability.

Fig. 7. An ORTEP diagram of the molecular structure of $Os_2(CO)_6(\mu-\eta^4-C_{24}H_{12})$ (5) showing 40% thermal ellipsoid probability.

Fig. 8. An ORTEP diagram of the molecular structure of $Os_2(CO)_5(\mu-\eta^4-C_{24}H_{12})(\eta^4-C_{12}H_8)$ (7) showing 40% thermal ellipsoid probability.

single bond between atoms C(52) and C(53), C(52)–C(53) = 1.472(10) Å. Carbon atoms C(51) and C(52) are π-bonded to Os(1). Atoms C(53) and C(54) are π-bonded to Os(3). There is a hydrogen atom on atom C(54), $\delta = 4.19$ ppm which exhibits long range coupling, $^3J_{H-H} = 1.5$ Hz, to the hydride ligand, $\delta = -18.09$ ppm in the ^{1}H-NMR spectrum. The hydride ligand was also located and refined crystallographically and found to bridge the Os(2)–Os(3) bond.

ORTEP diagrams of the diosmium cluster complexes 5 and 7 are shown in Figs. 7 and 8, respectively. Selected bonds distances and angles for these compounds are shown in Table 5. Both compounds contain two coupled acenaphthyne molecules that bridge the two metal atoms to form a metallacycle similar to the ferrole structures formed by the coupling of alkynes by iron carbonyl [29]. Electron counting indicates that the metal–metal bond is a donor:acceptor bond from Os(1) to Os(2). Compound 7 differs from 5 by the
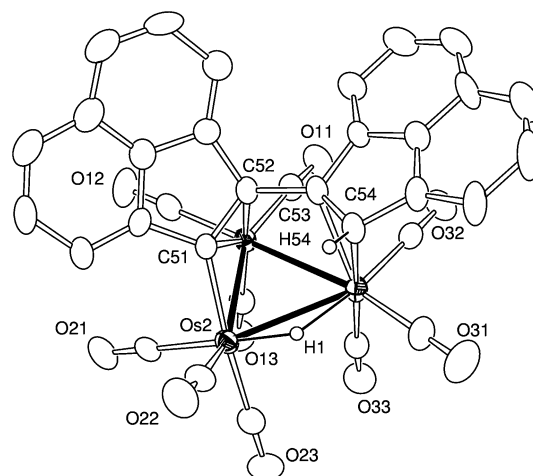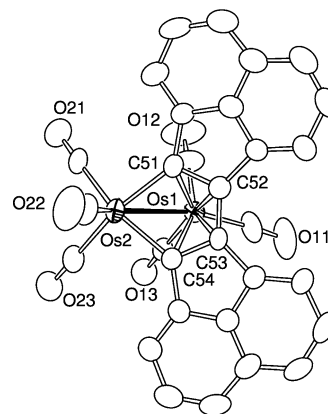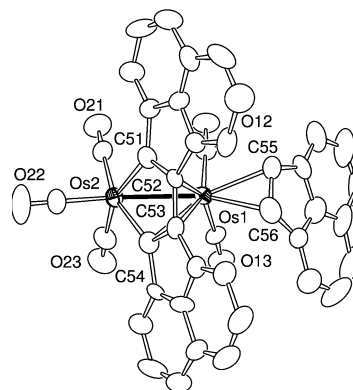
presence of an acenaphthlene ligand that has been substituted for one of the CO ligands in 5. This ligand is π-bonded to the metal atom Os(1). Compound 6 is a
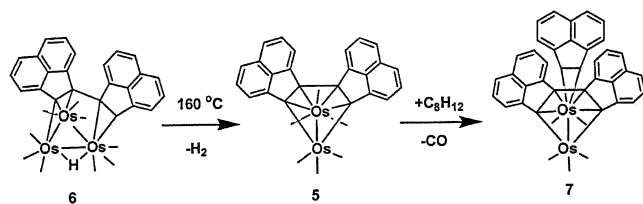
Scheme 2.

Table 5
Selected intramolecular distances and angles for compounds **5** and **7** [a]

Compound **5**		Compound **7**	
Bond distances (Å)			
Os(1)–C(52)	2.288(6)	Os(1)–C(56)	2.274(9)
Os(1)–C(53)	2.299(6)	Os(1)–C(52)	2.282(9)
Os(1)–C(51)	2.312(5)	Os(1)–C(55)	2.301(10)
Os(1)–C(54)	2.335(6)	Os(1)–C(51)	2.307(9)
Os(1)–Os(2)	2.7599(3)	Os(1)–C(53)	2.315(9)
Os(2)–C(51)	2.083(5)	Os(1)–C(54)	2.329(10)
Os(2)–C(54)	2.099(5)	Os(1)–Os(2)	2.7480(5)
C–O (av)	1.13(1)	Os(2)–C(54)	2.083(9)
		Os(2)–C(51)	2.096(9)
		C–O (av)	1.14(1)
Bond angles (°)			
C(52)–Os(1)–Os(2)	73.49(14)	C(56)–Os(1)–Os(2)	156.5(3)
C(53)–Os(1)–Os(2)	73.25(12)	C(52)–Os(1)–Os(2)	73.8(2)
C(51)–Os(1)–Os(2)	47.50(13)	C(55)–Os(1)–Os(2)	157.7(3)
C(54)–Os(1)–Os(2)	47.77(13)	C(51)–Os(1)–Os(2)	48.0(2)
C(51)–Os(2)–Os(1)	54.90(15)	C(53)–Os(1)–Os(2)	73.6(2)
C(54)–Os(2)–Os(1)	55.46(15)	C(54)–Os(1)–Os(2)	47.6(2)

[a] Estimated S.D.s in the last significant figure are given in parentheses.

precursor to **5** and it is converted into **5** in 40% yield when it is heated to 160 °C for a period of 5 h (see Scheme 2).

The principal difference between the reactions of acenaphthylene with triiron dodecacarbonyl and triruthenium dodecacarbonyl with that of $Os_3(CO)_{10}$-$(NCMe)_2$ reported here is that CH activation does not occur with the former compounds, while CH activation occurs exclusively with the osmium compound (see Scheme 1). Acenaphthylene has been shown to be a precursor to decacyclene which in turn can be converted into bucky bowls [23]. In this work we have shown that triosmium cluster complexes can convert acenaphthylene to acenaphthyne complexes by selectively activating the C–H bonds on the five membered ring. Furthermore, we have shown that the clusters can activate two acenaphthylene molecules and couple them. These could be precursors to other carbon-rich organometallic complexes and polycyclic aromatic hydrocarbons.

4. Supplementary material

X-ray crystallographic data in CIF format have been deposited with the Cambridge Crystallographic Data Centre, CCDC nos. 213490–213495 for compounds **2**–**7**. Copies of this information may be obtained free of charge from The Director, CCDC, 12 Union Road, Cambridge CB2 1EZ, UK (Fax: +44-1223-336033; e-mail: deposit@ccdc.cam.ac.uk or www: http://www.ccdc.cam.ac.uk).

References

[1] E.O. Fischer, K. Ofele, Chem. Ber. 90 (1957) 2532.
[2] R.J. Dellace, B.R. Penfold, Inorg. Chem. 11 (1972) 1855.
[3] R. Mason, W.R. Robinson, J. Chem. Soc. Chem. Commun. (1968) 468.
[4] S. Brait, S. Deabate, S.A.R. Knox, E. Sappa, J. Cluster Sci. 12 (2001) 139.
[5] M.R. Churchill, W.J. Youngs, Inorg. Chem. 18 (1979) 1697.
[6] M.A. Bennett, K.D. Griffiths, T. Okano, V. Parthasarathi, G.B. Robertson, J. Am. Chem. Soc. 112 (1990) 7047.
[7] E.L. Muetterties, J.R. Bleeke, E.J. Wucherer, Chem. Rev. 82 (1982) 499.
[8] R.J. Goudsmit, B.F.G. Johnson, J. Lewis, P.R. Raithby, M.J. Rosales, J. Chem. Soc. Dalton Trans. (1983) 2257.
[9] W.Y. Yeh, S.C.N. Hsu, S.-M. Peng, G.H. Lee, Organometallics 17 (1998) 2477.
[10] A.J. Arce, K. Arquimedes, Y.D. Sanctis, M.V. Capparelli, A.J. Deeming, Inorg. Chem. Acta. 285 (1999) 277.
[11] W.R. Cullen, S.J. Rettig, R. Zheng, Organometallics 11 (1992) 928.
[12] S.C. Brown, J. Evan, L.E. Smart, J. Chem. Soc. Chem. Commun. (1980) 1021.
[13] R.D. Adams, N.M. Golembeski, J. Organomet. Chem. 172 (1979) 239.
[14] R.D. Adams, D.A. Katahira, L.-W. Yang, Organometallics 1 (1982) 235.
[15] W.K. Leong, G. Chen, Organometallics 20 (2001) 2280.
[16] D.B. Brown, B.F.G. Johnson, C.M. Martin, A.E.H. Wheatley, J. Chem. Soc. Dalton Trans. (2000) 2055.
[17] H. Chen, M. Fajardo, B.F.G. Johnson, J. Lewis, P.R. Raithby, J. Organomet. Chem. 389 (1990) C16.
[18] A.J. Deeming, A.J. Arce, Y. De Sanctis, M.W. Day, K.I. Hardcastle, Organometallics 8 (1989) 1408.
[19] R.D. Adams, X. Qu, Organometallics 14 (1995) 2238.
[20] A.J. Deeming, Adv. Organomet. Chem. 26 (1986) 1.
[21] (a) R.B. King, F.G.A. Stone, J. Am. Chem. Soc. 82 (1960) 4557;
(b) R.B. King, F.G.A. Stone, J. Am. Chem. Soc. 88 (1966) 2075;
(c) M.R. Churchill, J. Wormald, Inorg. Chem. 9 (1970) 2239.
[22] H. Nagashima, T. Fukahori, K. Aoki, K. Itoh, J. Am. Chem. Soc. 115 (1993) 10430.
[23] (a) L.T. Scott, M.S. Bratcher, S. Hagen, J. Am. Chem. Soc. 118 (1996) 8743;
(b) R.B.M. Ansems, L.T. Scott, J. Am. Chem. Soc. 122 (2000) 2719.

[24] K. Dziewonski, Chem. Ber. 36 (1903) 962.

[25] K. Zimmerman, M.W. Haenel, Synlett 5 (1997) 610.

[26] S.R. Drake, R. Khattar, Org. Synth. 4 (1988) 234.

[27] SAINT+, version 6.02a, Bruker Analytical X-ray Systems, Inc., Madison, WI, 1998.

[28] G.M. Sheldrick, SHELXTL, Version 5.1, Bruker Analytical X-ray Systems, Inc., Madison, WI, 1997.

[29] W.P. Fehlhammer, H. Stolzenberg, in: G. Wilkinson, F.G.A. Stone, E.W. Abel (Eds.), Comprehensive Organometallic Chemistry, vol. 4 (Section 31.4.2.2.4), Pergamon, Oxford, 1982 .